

INFLUENCE OF B AND ZR ON MICROSTRUCTURE AND MECHANICAL PROPERTIES OF ALLOY 718

T. Fedorova¹, J. Rösler¹, B. Gehrmann² and J. Klöwer²

¹Technische Universität Braunschweig, D-38106 Braunschweig

²ThyssenKrupp VDM GmbH, D-58791 Werdohl

Keywords: Alloy 718, B, Zr, microstructure

Abstract

The basic intent of this paper is to examine the role of the minor elements B and Zr within typical specification limits for alloy 718 with respect to (i) microstructure evolution, (ii) strengthening effects and (iii) thermal stability. For this purpose, thermodynamic calculations using the software THERMOCALC were performed, varying the content of B and Zr. In addition, alloys with precisely controlled chemical composition (with content variations of 20 to 100ppm B and/or of 50 to 200ppm Zr) were prepared by drop casting in a vacuum arc furnace and hot forged, so that it was possible to compare the theoretical predictions with experimental results. The microstructure evolution was studied in detail by means of scanning electron microscopy (SEM) and x-ray diffraction. Furthermore, mechanical properties including tensile and creep behaviour were examined. Based on these results, dependencies between chemical composition, microstructure and mechanical properties will be elucidated.

Introduction

The strength of Fe-Ni-based superalloys is dependent on several factors, such as solid solution strengthening, volume fraction and size of the precipitates. Since these factors are controlled by the composition of each phase, numerous studies have been carried out on the partitioning behavior of alloying elements between the γ , γ' and γ'' phases [1].

The influence of minor elements, especially B, on the mechanical properties of Alloy 718 and its derivatives was studied in many works in the last years [2-7, 12]. It was realized that small additions of B and Zr were extremely beneficial to the creep-rupture properties of nickel-base superalloys. In the late 1950s, it was reported that B (up to 0.01 pct) and Zr (up to 0.1 pct) improved high-temperature strength, ductility, and notch sensitivity of several alloys. In the study of Floreen and Davidson the influence of B and Zr on the creep and fatigue crack growth behavior of Ni-base superalloys was shown. They realized that additions of B and Zr markedly improved the smooth specimen creep properties and the threshold stress intensity values for creep crack growth [8].

In another study it was shown that B and C strongly influenced the formation of grain boundary precipitates, and B causes the formation of an intergranular M_3B_2 boride. Both, B and Zr, were observed to be critical for improvement of the mechanical properties of the superalloys [9]. Recently, Cao and Kennedy have proposed to add B and P and showed that B and P increased the resistance to creep deformation [10]. The effect on creep strength of Alloy 718 due to addition of both elements was more visible than the effect due to their separate addition.

B and Zr positively affect the creep properties of complex nickel-base heat-resistant alloys. Their addition decreases the tendency to microcracking allowing longer creep exposure and higher creep deformations [11].

However, it has not been investigated in many studies how the addition of B and Zr influences the microstructure of Alloy 718 (grain coarsening and morphology of δ -Ni₃Nb phase). This paper seeks to define the role of B and Zr in forming the microstructure of Alloy 718 with the aim to improve its microstructural stability and strength.

Experimental Procedures

The alloys studied in this paper were made by induction melting under an Ar atmosphere (alloy 1) and by plasma arc melting, followed by casting the material into a water-cooled copper crucible (alloys 2-6). Their nominal chemical compositions are given in Table I. The Nb concentration of alloy 1 was taken in the limits of the ASTM specification and SAE AMS for Alloy 718. The B concentration is limited to 60 ppm. The Zr concentration is not indicated. The alloy 1 was melted without additions of B or Zr in order to take its microstructure as the reference. All alloys were homogenized at 1140 °C/6 h + 1175 °C/20 h in vacuum.

The alloys 2-6 with additions of B and Zr were deformed from 13 mm to 9 mm by rotary swaging at 1075 °C. The resulting rods were solution annealed at 980 °C/ 1.5 h, followed by water cooling to room temperature (RT). The material was then double aged at 721 °C/ 8 h + furnace cooled at 50 °C/h + 620 °C/8 h air cooled to RT.

In order to predict the phases in the alloys, ThermoCalc software version S and the commercial TTNi7 database were used to calculate the phases and their precipitation temperatures. The phases considered in the calculation were face centered cubic γ , L1₂-ordered γ' , DO₂₂-ordered γ'' , σ , Laves, MC, M₆C, M₃B₂, MB₂ and liquid. It was necessary to suppress the orthorhombic Ni₃Nb δ phase from the calculations due to its interference with the γ'' phase and vice versa.

Table I. Nominal chemical compositions of alloys

Alloy	C	Ni	Cr	Fe	Mo	Nb	Ti	Al	B	Zr
ASTM Spec.	Max 0.08	50-55	17-21	balance	2.80-3.30	4.75-5.50	0.65-1.15	0.20-0.80	Max 60ppm	-
Alloy 1	0.025	balance	18.7	17	2.96	5.37	0.96	0.48	-	-
Alloy 2	0.025	balance	18.7	17	2.96	5.4	0.96	0.48	60ppm	-
Alloy 3	0.025	balance	18.7	17	2.96	5.38	0.96	0.48	150ppm	-
Alloy 4	0.025	balance	18.7	17	2.96	5.41	0.96	0.48	200ppm	-
Alloy 5	0.025	balance	18.7	17	2.96	5.39	0.96	0.48	60ppm	200ppm
Alloy 6	0.025	balance	18.7	17	2.96	5.37	0.96	0.48	100ppm	200ppm

The first microstructure preparation was made using Murakami etching reagent in order to evaluate the amount and the morphology of carbides, carbo-nitrides and borides. The Murakami etching reagent etches selectively the precipitates of carbides, carbo-nitrides and borides and does not affect the matrix. The chemical composition of Murakami etching reagent is 100 ml H₂O, 10 g KOH (or NaOH) and 10 g K₃[Fe(CN)₆].

The V2A etching reagent was used during the second microstructure preparation. It was possible to identify the morphology of γ' , γ'' , δ , σ , Laves and carbides because the matrix was selectively etched in contrast to the precipitates named above. With help of this etching reagent, the grain boundaries and respectively grain sizes could also be identified. The chemical

composition of the V2A etching reagent is 200 ml H₂O, 200 ml HCl, 20 ml HNO₃ and 0,6 ml “Vogels Sparbeize”.

SEM was used to observe the morphology and the distribution of all the phases. The chemical composition of the precipitates was identified by means of EDX.

Experimental Results

The thermodynamic prediction of the phase's solvus temperature in case of the solid phases and the solidus temperature in case of the liquid phase for alloy 1 with addition of boron is shown in Fig.1.

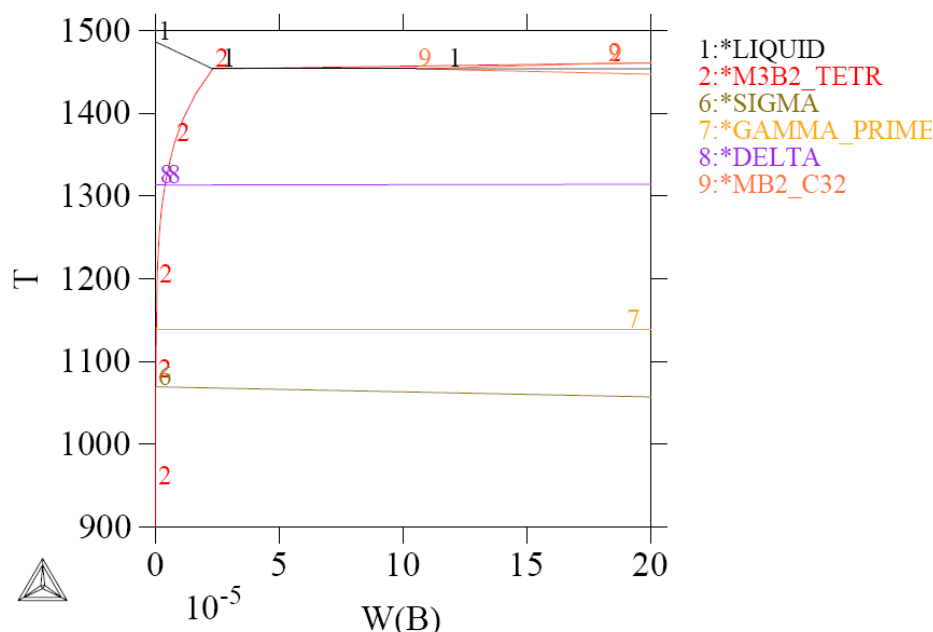


Fig.1. ThermoCalc calculations for alloy 1 with B addition up to 200 ppm

The boron concentration was varied up to 200ppm. The Ni concentration was balanced; the other elements stayed constant. An increase of boron amount to approximately 40ppm raises the solvus temperature and stability of the M₃B₂ phase. Further additions of boron did not influence the solvus temperature of M₃B₂ phase. The phase MB₂ precipitates at boron concentrations above about 65ppm. The solvus temperature of this phase remains constant according to the calculations. The volume fractions of both phases are very small because of the low boron content.

The same thermodynamical calculations were made for alloy 1 with additions of Zr. The calculation showed that Zr additions up to 200ppm did not have any effect.

Grain boundary precipitation of δ -Ni₃Nb (in short rods and globular morphology) and grain boundary precipitation of carbides are typical for the microstructure of Alloy 718 (see Fig. 2). The main fine precipitations of disk-like γ'' and precipitations of fine globular γ' can not usually be detected in the SEM.

Carbides and carbo-nitrides (dark angular precipitates) in Fig. 2a and 2b are much coarser than the plate like δ -Ni₃Nb phase precipitates at the grain boundaries (Fig. 2b and 2c.). With help of energy-dispersive spectroscopy (EDS), the carbo-nitrides (Fig. 2a) could be identified (Fig. 3).

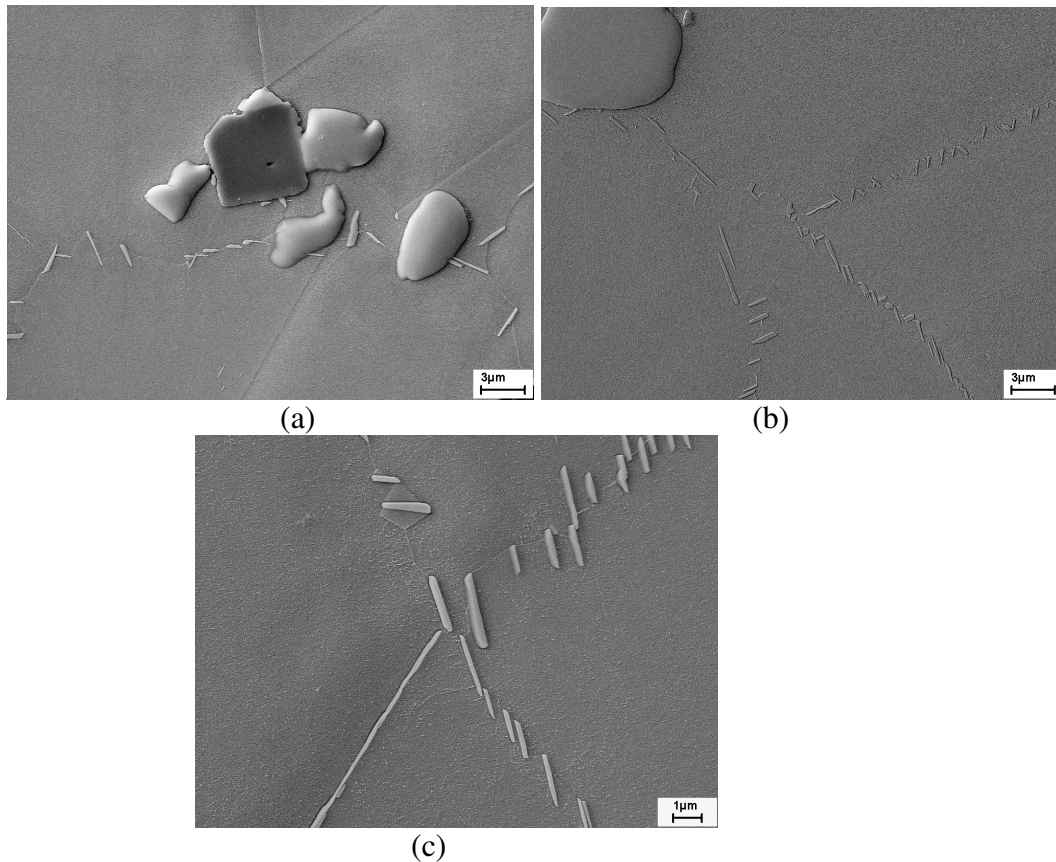


Fig.2. Microstructures of alloy 1 (V2A etching reagent), showing large carbides and carbo-nitrides (a, b) and δ -Ni₃Nb phase at grain boundaries (a-c)

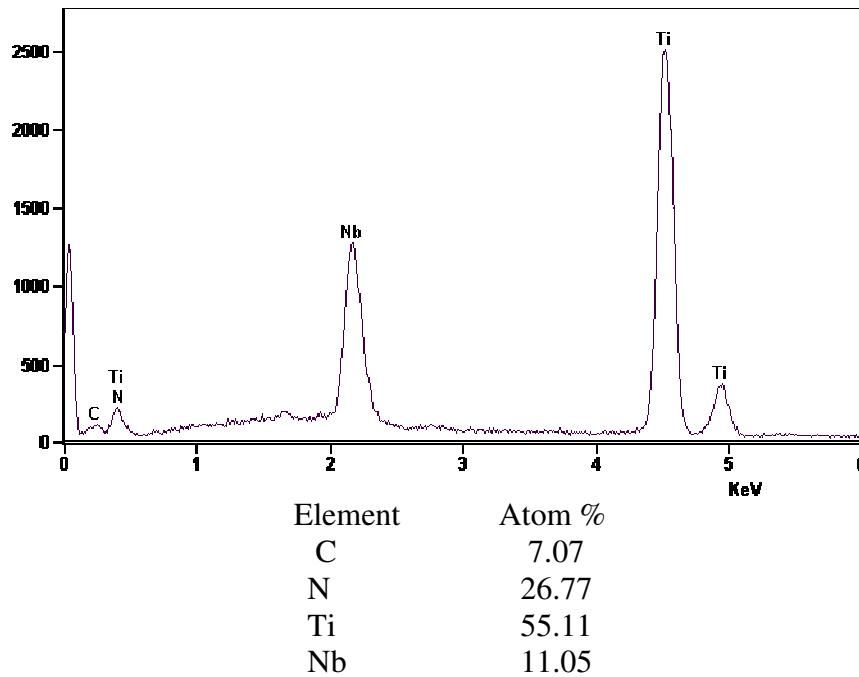


Fig.3. EDS spectrum of carbo-nitride (dark angular precipitate in Fig. 2a)

Investigation of alloys 2-6 demonstrated that boron has a large influence on castability. All solidification rods of alloys 3 and 4 with 150ppm B and 200ppm B respectively showed cracks in their middle part after melting and casting into a water-cooled copper mould (Fig. 4a) and could not be deformed. Obviously, these alloys are sensitive to hot cracking due to high concentration of B (Fig. 4b). The fracture morphology is shown in Fig. 4 (b-d) at higher magnification. It is typical far hot tearing, often exposing dendrite arms.

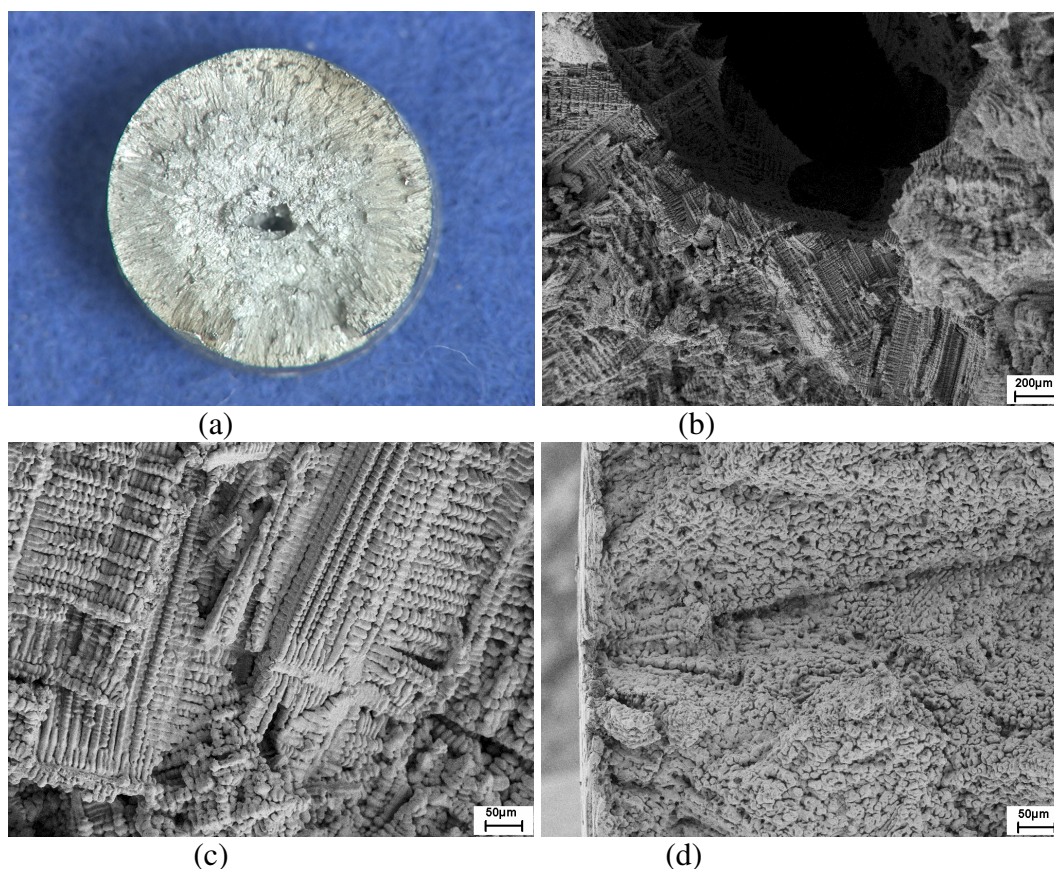


Fig.4. Cracked rod of alloy 4 (a) and corresponding SEM micrographs close to the central cavity (b, c) and to the specimen surface (d)

The microstructure of alloy 2 (60ppm B), alloy 5 (60ppm B, 200ppm Zr) and alloy 6 (100ppm B, 200ppm Zr) is shown in Fig. 5. The SEM micrographs show clearly that the volume fraction of etched precipitates increases from alloy 2 (Fig. 5 a-b) to alloy 5 (Fig. 5 b-c) and 6 (Fig. 5 d-e). As a boride creator, zirconium increases the amount of $(\text{Nb,Ti,Zr})_x\text{B}_y$ borides (Fig. 5 b-c). EDS analysis of alloy 5 verifies this conclusion (Fig. 6). Zirconium in Alloy 718 has also a big influence on precipitates at grain boundaries. Fig. 5 e-f demonstrates that a large area along grain boundaries was selectively etched, which can be attributed to the $\delta\text{-Ni}_3\text{Nb}$ phase.

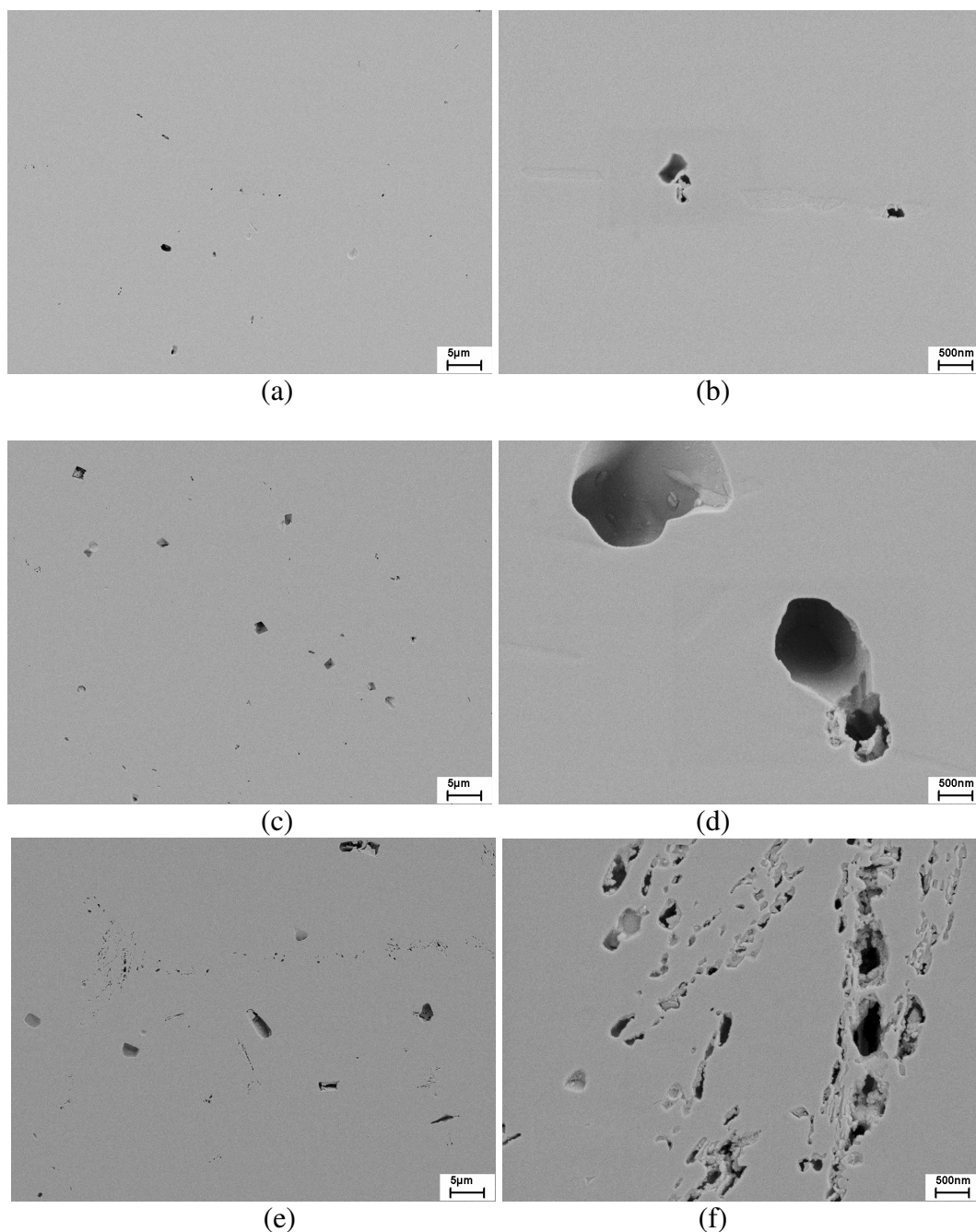


Fig.5. Microstructures of alloy 2 (60ppm B) (a-b), alloy 5 (60ppm B and 200ppm Zr)(c-d) and alloy 6 (100ppm B and 200ppm Zr) (e-f)

For further phase analysis the samples were also etched with V2A etchant, revealing the δ -Ni₃Nb phase as well as carbides, boride and carbo-nitride. In case of alloy 2 (60ppm B, no Zr) the morphology of the precipitates is as exerted for Alloy 718 (Fig. 7a, b). Thus, the effect of small boron additions on the microstructure is limited to the formation of isolated borides as discussed above. However, when zirconium is added the result is vastly different. Alloys 5 and 6, containing 200ppm zirconium at essentially unaltered boron content, exhibit agglomerates of the δ -Ni₃Nb phase and its volume fraction increases significantly (Fig. 7c-e). EDS analysis (Fig. 8) confirms the critical role of zirconium, which strongly partitions to the δ -Ni₃Nb phase.

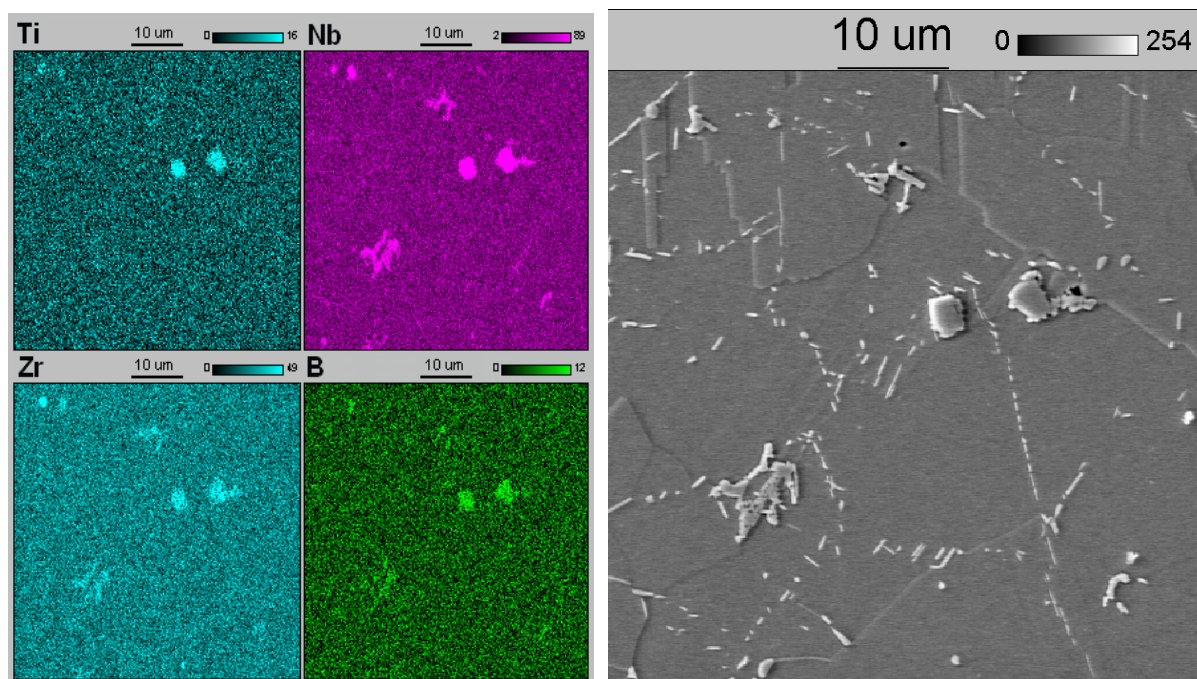
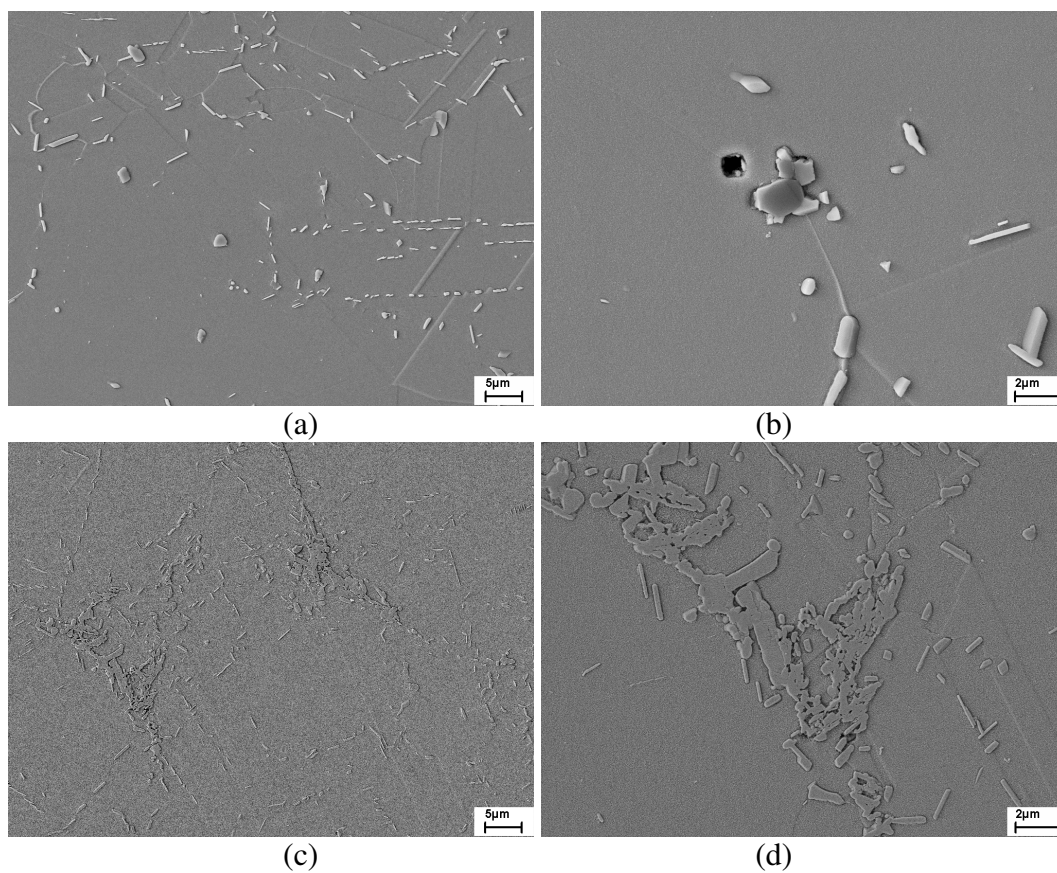


Fig.6. Microstructure of alloy 5 with corresponding EDS maps for niobium, titanium, zirconium and boron



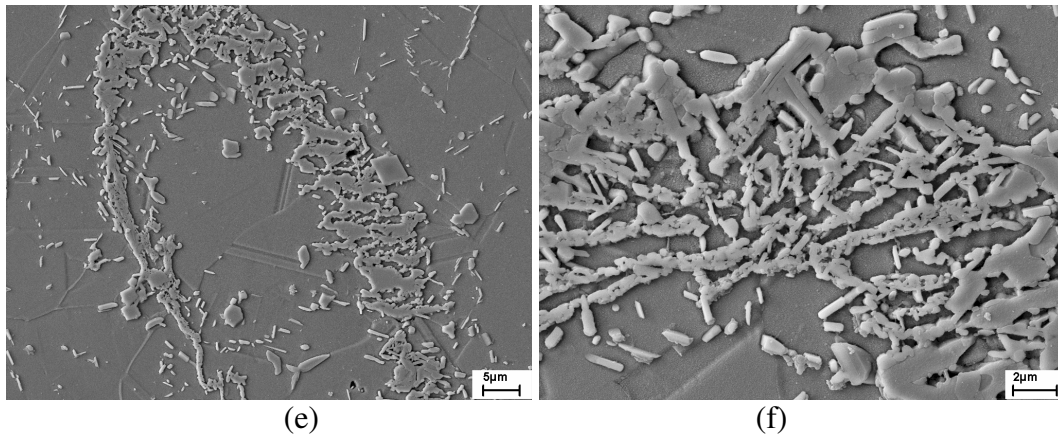


Fig.7. Microstructure of alloy 2 (a-b), alloy 5 (c-d) and alloy 6 (f-e)

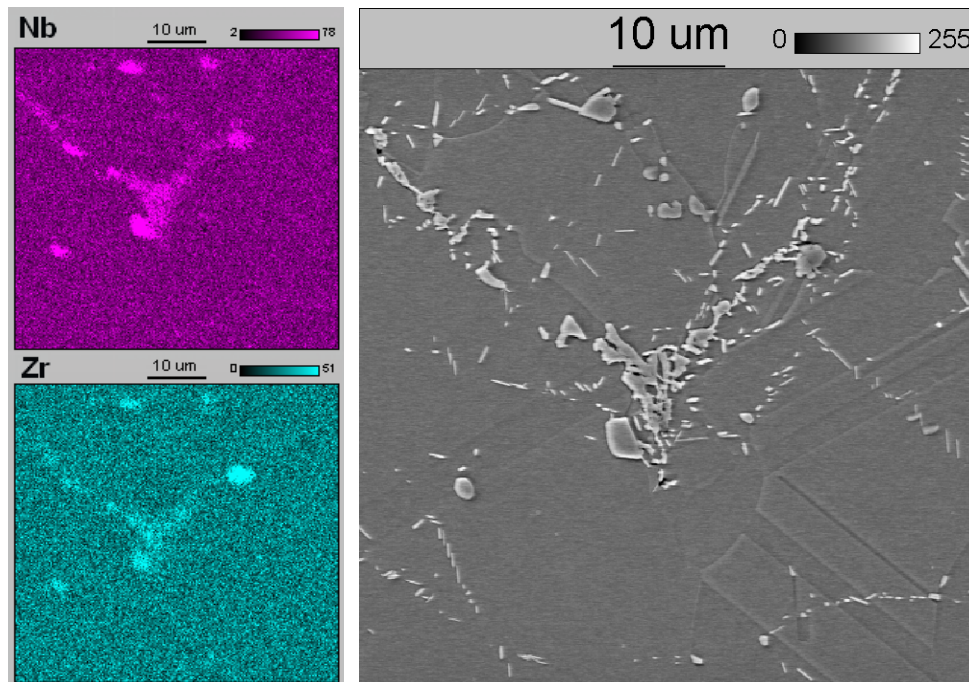


Fig.8. Microstructure of alloy 5 with corresponding EDS maps for niobium and zirconium

Summary

The results of this work show that even small changes in the concentration of the elements B and Zr in the Alloy 718 have large influence on its microstructure:

- Boron addition leads to the formation of borides in the microstructure while the morphology of all other phases remains unchanged.
- Boron concentrations beyond about 100ppm strongly increase the tendency to hot cracking of alloy 718 and therefore not advisable.
- The addition of zirconium strongly changes the morphology and volume fraction of borides and δ -Ni₃Nb phase, leading to large agglomerates, which are expected to

adversely affect mechanical properties. Hence, the zirconium content should be kept below 200ppm.

References

1. C.C. Jia, K. Ishida, and T. Nishizawa, Partition of Alloying Elements between γ (Al), γ' (L12), and β (B2) Phases in Ni-Al Base Systems, *Metallurgical and Materials Transactions*, Volume 25A, 473-482, (1994).
2. S. Benhadad, N.L. Richards, and M.C. Chaturvedi, The Influence of Minor Elements on the Weldability of an INCONEL 718-Type Superalloy, *Metallurgical and Materials Transactions*, Volume 33A, 2005-2012, (2002).
3. W. Chen, M.C. Chaturvedi, N.L. Richards, and G. McMahon, Grain Boundary Segregation of Boron in INCONEL 718, *Metallurgical and Materials Transactions*, Volume 29A, 1947-1954, (1998).
4. S.J. Sijbrandij, M.K. Miller, J.A. Horton, W.D. Cao, Atom Probe Analysis of Nickel-Based Superalloy IN-718 With Boron and Phosphorus Additions, *Materials Science and Engineering*, A250, 115-119, (1998).
5. W.R. Sun, S.R. Guo, J.H. Lee, N.K. Park, Y.S. Yoo, S.J. Choe, Z.Q. Hu, Effects of Phosphorus on the δ -Ni₃Nb Phase Precipitation and the Stress Rupture Properties in Alloy 718, *Materials Science and Engineering*, A247, 173-179, (1998).
6. L. Xiao, D.L. Chen, M.C. Chaturvedi, Effect of Boron and Carbon on Thermomechanical Fatigue of IN 718 Superalloy Part I. Deformation Behavior, *Materials Science and Engineering*, A437, 157-171, (2006).
7. L. Xiao, D.L. Chen, M.C. Chaturvedi, Effect of Boron and Carbon on Thermomechanical Fatigue of IN 718 Superalloy Part II. Deformation Microstructures, *Materials Science and Engineering*, A437, 172-182, (2006).
8. S. Floreen and J.M. Davidson, The Effects of B and Zr on the Creep and Fatigue Crack Growth Behavior of a Ni-Base Superalloy, *Metallurgical Transactions*, Volume 14A, 895-901, (1983).
9. T.J. Garosshen, T.D. Tillman, and G.P. McCarthy, Effects of B, C, and Zr on the Structure and Properties of P/M Nickel Base Superalloy, *Metallurgical Transactions*, Volume 18A, 69-77, (1987).
10. X. Xio, G. Wang, J. Dong, C. Xu, W.-D. Cao, R. Kennedy, Structure Stability Study on a Newly Developed Nickel-base Superalloy – ALLVAC 718Plus, *Superalloys 718, 625, 706 and Derivatives 2005*, 179-191, (2005).
11. X. Xie, J.Dong, G. Wang, W. You, The Effect of Nb, Ti, Al on Precipitation and Strengthening Behavior of 718 Type Superalloys, *Superalloys 718, 625, 706 and Derivatives 2005*, 287-298, (2005).

12. J. Rösler, S. Müller, Protection of Ni-Base Superalloys Against Stress Accelerated Grain Boundary Oxidation (SAGBO) by Grain Boundary Chemistry Modification, *Scripta Materialia*, Volume 40, 257-263, (1999).